Noise and Loss in Balanced and Subharmonically Pumped Mixers: Part II—Application

ANTHONY R. KERR, SENIOR MEMBER, IEEE

Abstract—**The theory presented in Part I is applied here to some simple two-diode subharmonically pumped and balanced mixers. It is shown that the magnitude of the loop inductance (seen by currents circulating through the two diodes) affects the subharmonically pumped mixer much more strongly than the balanced mixer. The theory is also applied to the ideal two-diode mixer (balanced or subharmonically pumped) using exponential diodes with no series resistance and no nonlinear capacitance. It is shown that, like its single-diode counterpart, this mixer has a noise-equivalent lossy network whose physical temperature is $\eta T/2$, where η is the ideality factor of the exponential diodes. It follows that the ideal subharmonically pumped resistive mixer is not intrinsically less noisy than the ideal resistive fundamental mixer. This is not necessarily the case if parametric effects, due to nonlinear diode capacitance, are present.**

I. Introduction

In PART I [1] the theory of subharmonically pumped and balanced mixers was given in a form suitable for solution by digital computer. In this part the application of the theory to practical mixers is demonstrated, and the properties of some two-diode mixers are examined. Of particular interest to the mixer designer are the effects of the loop inductance (seen by currents circulating through the two diodes) and the diode capacitance. In Section II, these effects are studied for a number of simple subharmonically pumped and balanced mixers.

Recent reports [2], [3] of excellent performance in subharmonically pumped mixers have led to speculation that they might be inherently less noisy than fundamental mixers. In Section IV it is shown that when ideal resistive diodes (with shot noise but no nonlinear capacitance) are used, this is not so.

II. Analysis of Some Two-Diode Mixers

In this section the simple subharmonically pumped and balanced mixer circuits shown in Figs. 1 and 2 are analyzed for various values of loop inductance and diode capacitance. The diodes are assumed to be of the Schottky barrier type, characterized in the usual way by

$$i_g = i_0\left[\exp\left(\alpha v_j\right) - 1\right] \tag{1}$$

and

$$\mathcal{C} = \mathcal{C}_0\left(1 - v_j/\phi\right)^{-\gamma} \tag{2}$$

where

$$\alpha = q/\eta kT. \tag{3}$$

Manuscript received March 23, 1979; revised August 8, 1979.

The author is with NASA Goddard Institute for Space Studies, Goddard Space Flight Center, New York, NY 10025.

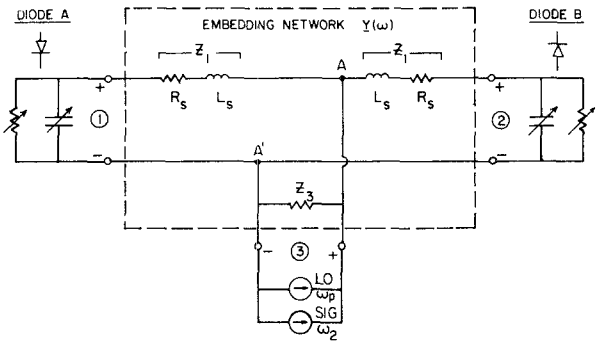

Fig. 1. Circuit of the subharmonically pumped mixer used in examples 1–4. The diodes are connected with opposite polarity so they conduct on alternate half-cycles of the LO. The series resistance R_s of the diodes is considered part of the embedding network. Z_3 represents the source or load impedance and depends on frequency, as indicated in Table I. In practice Z_3 would consist of a number of source or load impedances connected to AA' by filter circuits which separate the various sidebands and LO harmonics. The IF load $Z_3(\omega_0)$ is conjugate-matched to the output impedance of the mixer.

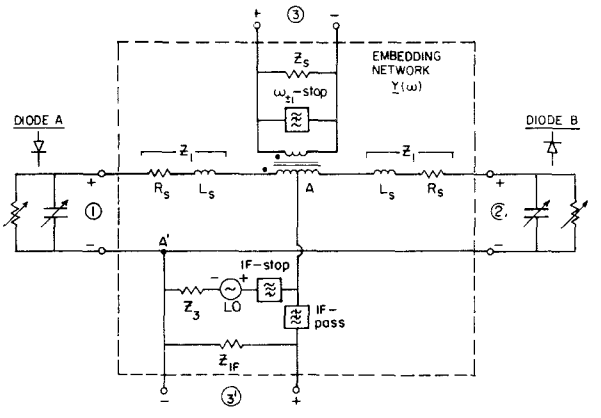

Fig. 2. Circuit of the balanced mixer used in examples 5 and 6. The diodes are connected with opposite polarity so they conduct on alternate half-cycles of the LO. The series resistance R_s of the diodes is considered part of the embedding network. Z_S is the source impedance at the signal and image frequencies $\omega_{\pm 1}$, and Z_3 is the LO source impedance. Because of the symmetry of the circuit, Z_3 is seen only by odd LO harmonics and even-order sidebands $\omega_{\pm 2}, \omega_{\pm 4}$, etc. Z_{IF} is the IF load impedance which is conjugate-matched to the output impedance of the mixer.

They exhibit shot noise due to the current i_g across the depletion layer, and thermal noise associated with the series resistance R_s.

A. Nonlinear Analysis

As seen by the local oscillator (LO) the circuits of Figs. 1 and 2 are symmetrical except for the opposite polarity of

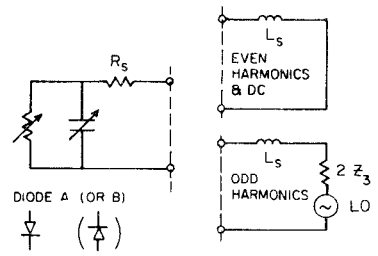

Fig. 3. The mixer circuits of Figs. 1 and 2 as seen by either diode at the LO frequency and its harmonics. The symmetry of the original circuits enables the diode conductance and capacitance waveforms to be determined as for a single-diode mixer.

the two diodes. The large-signal current and voltage waveforms at the diodes are therefore opposite in polarity and have a delay of half an LO period with respect to one another. It follows that even-order LO harmonics (and dc) are out of phase at the two diodes, thereby producing zero voltage at AA' in Figs. 1 and 2, while odd harmonics at the two diodes are in phase. To determine the LO waveforms at either diode it is therefore sufficient to consider the single-diode circuit of Fig. 3, which is easily analyzed using the iterative multiple-reflection technique [4] discussed in the introduction to Part I. In the following examples the LO power is adjusted to give a rectified current of 2 mA (±2 percent) in each diode, with zero dc bias voltage.

B. Small-Signal and Noise Analysis

Examples 1 to 4—Subharmonically Pumped Mixer: At any frequency ω the embedding network of the subharmonically pumped mixer in Fig. 1 can be represented by its admittance matrix

$$\boldsymbol{Y}(\omega)=\frac{1}{Z_1}\begin{bmatrix}1 & 0 & -1\\ 0 & 1 & -1\\ -1 & -1 & 2+Z_1/Z_3\end{bmatrix} \tag{4}$$

where $Z_1(\omega)=R_S+j\omega L_S$. From this it is possible to construct the admittance matrix $\boldsymbol{Y}^E$ of the multifrequency embedding network [1, Fig. 3]. Typical elements of $\boldsymbol{Y}^E$ are

$$\left.\begin{aligned} Y^E_{(A,n)(A,n)}&=Y_{11}(\omega_n), & Y^E_{(A,m)(A,n)}&=0\\ Y^E_{(A,n)(B,n)}&=Y_{12}(\omega_n), & Y^E_{(A,m)(B,n)}&=0\\ Y^E_{(A,n)(C,n)}&=Y_{13}(\omega_n), & Y^E_{(A,m)(C,n)}&=0\\ &\vdots & &\vdots \end{aligned}\right\}. \tag{5}$$

From the large-signal analysis the admittance matrices $\boldsymbol{Y}^A$ and $\boldsymbol{Y}^B$ of the two pumped diodes can be formed using [1, eq. (12)]

$$\left.\begin{aligned} Y^A_{m,n}&=G^A_{m-n}+j\omega_m C^A_{m-n}\\ Y^B_{m,n}&=G^B_{m-n}+j\omega_m C^B_{m-n}. \end{aligned}\right\} \tag{6}$$

In these examples eight harmonics of the LO were determined by the nonlinear analysis, allowing size 9×9 matrices $\boldsymbol{Y}^A$ and $\boldsymbol{Y}^B$ to be used. The effects of the matrix size are discussed in Section III.

The mixer admittance matrix $\boldsymbol{Y}^M$ can now be formed by adding $\boldsymbol{Y}^A$ and $\boldsymbol{Y}^B$ to $\boldsymbol{Y}^E$ according to [1, eq. (14)]. $\boldsymbol{Y}^E$ and $\boldsymbol{Y}^M$ are of size 27×27 in these examples.

The output impedance of the mixer is found by setting $Z_3(\omega_0)=\infty$ (Fig. 1), which gives $Z_{\text{out}}=Z^{Mo/c}_{(C,0)(C,0)}$, where $\boldsymbol{Z}^{Mo/c}=(\boldsymbol{Y}^{Mo/c})^{-1}$, as described in Part I. If the output of the mixer is conjugate-matched, the input impedance and conversion loss are [1, eqs. (22) and (20)]:

$$Z_{\text{in}_{\pm 2}}=\left[\frac{1}{Z^M_{(C,\pm 2)(C,\pm 2)}}-Y_{\pm 2}\right]^{-1} \tag{7}$$

$$L_{0,\pm 2}=\frac{1}{4\left|Z^M_{(C,0)(C,\pm 2)}\right|^2\text{Re}[Y_{\pm 2}]\text{Re}[Y_0]} \tag{8}$$

where the signal and image source admittances $Y_{\pm 2}=1/Z_3(\omega_{\pm 2})$, and the IF load admittance $Y_0=1/Z^*_{\text{out}}(\omega_0)$.

In determining the noise temperature of the mixer, thermal noise from the signal and image source conductances $\text{Re}[Y_{\pm 2}]$, and from the IF load conductance $\text{Re}[Y_0]$, should not be included. This is accomplished by using $\boldsymbol{Y}^{E(\text{unterm.})}$ in calculating the thermal noise contribution to the overall noise correlation matrix. In this example $\boldsymbol{Y}^{E(\text{unterm.})}$ is identical to $\boldsymbol{Y}^E$ except for three elements:

$$\left.\begin{aligned} Y^{E\ (\text{unterm})}_{(C,\pm 2)(C,\pm 2)}&=Y^E_{(C,\pm 2)(C,\pm 2)} & &-\text{Re}[Y_{\pm 2}]\\ Y^{E\ (\text{unterm.})}_{(C,0)(C,0)}&=Y^E_{(C,0)(C,0)} & &-\text{Re}[Y_0]. \end{aligned}\right\} \tag{9}$$

The noise correlation matrix $\boldsymbol{N}$ can now be determined using [1, eq. (36)], and from it the single sideband (SSB) input noise temperature of the mixer:

$$T_{M_{\pm 2}}=\frac{\boldsymbol{Z}^M_{(C,0)}\boldsymbol{N}\boldsymbol{Z}^{M\dagger}_{(C,0)}}{4k\,\text{Re}[Y_{\pm 2}]\cdot\left|Z^M_{(C,0)(C,\pm 2)}\right|^2\Delta f} \tag{10}$$

where $T_{M_{+2}}$ and $T_{M_{-2}}$ are the SSB input noise temperatures referred to the upper and lower sidebands.

The performance of the subharmonically pumped mixer of Fig. 1 was computed for the four sets of circuit parameters shown in Table I, examples 1–4. For each example the series inductance L_S was allowed to vary over a range of values to determine its effect. With each value of L_S the complete analysis, nonlinear and small signal, was performed. The signal, image, LO, and IF are at 103, 97, 50, and 3 GHz. The results are shown in Figs. 4–7. Typically 80 values of L_S were used in each set. Computation time using an IBM 360-95 was about 30 s per value of L_S. The results will be discussed in a later section, together with those of the balanced mixer examples.

Examples 5 and 6—Balanced Mixer: The analysis of the balanced mixer of Fig. 2 is similar to that of the subharmonically pumped mixer just described, with the signal and image frequencies now being $\omega_{\pm 1}$. At all sidebands except the IF (ω_0) the admittance matrix for ports 1, 2, and 3 of the embedding network is

$$\boldsymbol{Y}(\omega)=\frac{1}{Z_1(Z_1+2Z_3)}\cdot\begin{bmatrix}Z_1+Z_3 & -Z_3 & -(Z_1+2Z_3)\\ -Z_3 & Z_1+Z_3 & Z_1+2Z_3\\ -(Z_1+2Z_3) & Z_1+2Z_3 & (Z_1+2Z_3)(2+Z_1/Z_S)\end{bmatrix}. \tag{11}$$

TABLE I

Diode Parameters And Circuit Elements For Examples 1–6

Example #	Type	R_s	C_0	γ	Values of Z_3, Z_S, and Z_{IF}		
					ω_p, $2\omega_p$, $\omega_p \pm \omega_0$, $2\omega_p \pm \omega_0$	ω_0	Higher Freq's
1	SHP	10Ω	7fF	0.5	50Ω	Match	0
2	SHP	5Ω	14fF	0.5	50Ω	Match	0
3	SHP	10Ω	7fF	0.5	50Ω	Match	1000Ω
4	SHP	10Ω	7fF	0	50Ω	Match	1000Ω
5	BM	10Ω	7fF	0.5	50Ω	Match	50Ω
6	BM	10Ω	7fF	0	50Ω	Match	50Ω

For Subharmonically pumped (SHP) mixers: ω_p = 50 GHz, ω_0 = 3 GHz.
For balanced mixers (BM): ω_p = 100 GHz, ω_0 = 3 GHz.
For all examples: γ = 1.12, ϕ = 0.95V, $i_0 = 8 \times 10^{-17}$ A, and the LO power is adjusted to give a rectified current of 2 mA in each diode. No dc bias is applied.

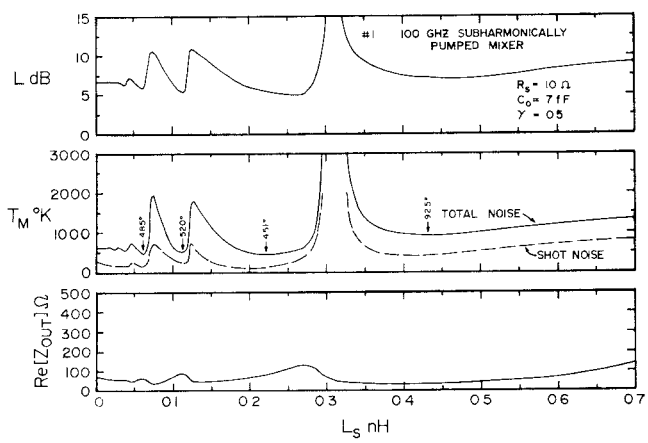

Fig. 4. Example 1: 100-GHz subharmonically pumped mixer of Fig. 1 with $Z_3 = 0$ for all frequencies beyond the signal and image, $\omega_{\pm 2}$. The conversion loss and equivalence input noise temperature, both SSB, and real part of the IF output impedance, are shown as functions of inductance L_S. Other details are given in Table I.

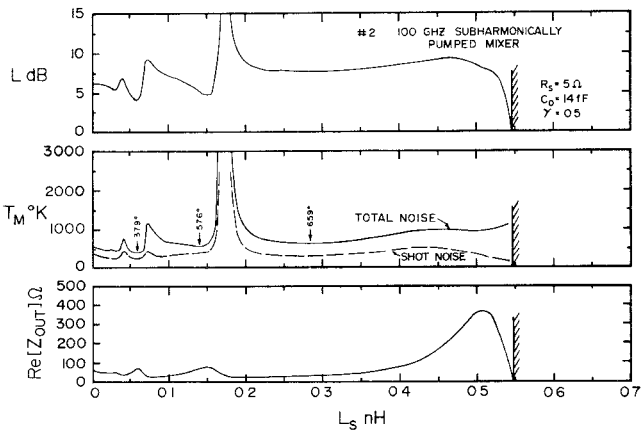

Fig. 5. Example 2: 100-GHz subharmonically pumped mixer of Fig. 1 with $Z_3 = 0$ for all frequencies beyond the signal and image, $\omega_{\pm 2}$. This is the same as example 1, except that larger diodes are used. The conversion loss and equivalent input noise temperature, both SSB, and real part of the IF output impedance, are shown as functions of inductance L_S. Other details are given in Table I.

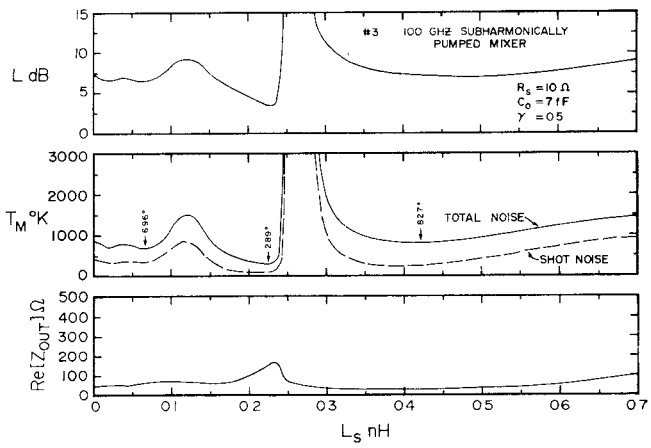

Fig. 6. Example 3: 100-GHz subharmonically pumped mixer of Fig. 1. This is the same as example 1, except that $Z_3 = 1000$ Ω for all frequencies beyond the signal and image, $\omega_{\pm 2}$. The conversion loss and equivalent input noise temperature, both SSB, and real part of the IF output impedance, are shown as functions of inductance L_S. Other details are given in Table I.

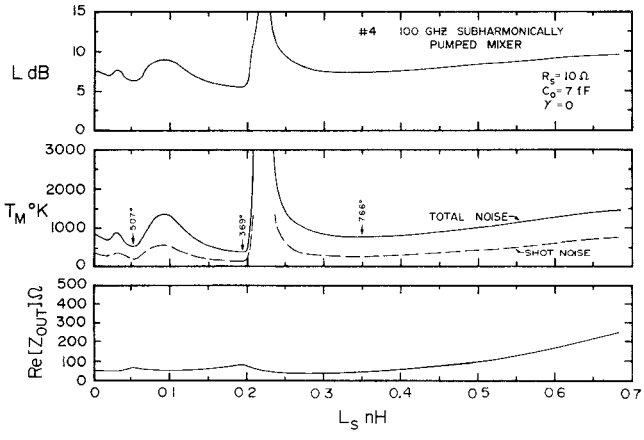

Fig. 7. Example 4: 100-GHz subharmonically pumped mixer of Fig. 1. This is the same as example 3, except that the diode capacitance is assumed independent of voltage ($\gamma = 0$). $Z_3 = 1000$ Ω for all frequencies beyond the signal and image, ω_{+2}. The conversion loss and equivalent input noise temperature, both SSB, and real part of the IF output impedance, are shown as functions of inductance L_S. Other details are given in Table I.

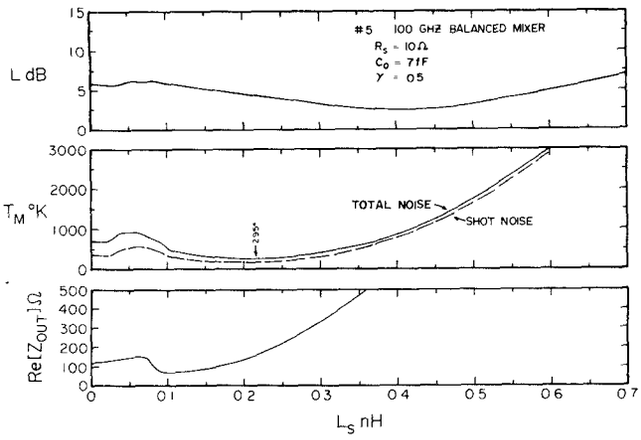

Fig. 8. Example 5: 100-GHz balanced mixer of Fig. 2. The signal and image source impedance Z_S and the LO source impedance Z_3 are all 50 Ω. The conversion loss and equivalent input noise temperature, both SSB, and real part of the IF output impedance, are shown as functions of inductance L_S. Other details are given in Table I.

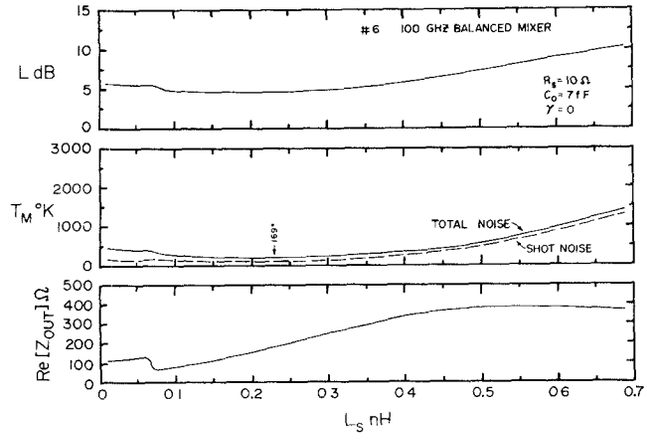

Fig. 9. Example 6: 100-GHz balanced mixer of Fig. 2. This is the same as example 5, except that the diode capacitance is assumed independent of voltage ($\gamma=0$). The signal and image source impedance Z_S and the LO source impedance Z_3 are all 50 Ω. The conversion loss and equivalent input noise temperature, both SSB, and real part of the IF output impedance, are shown as functions of inductance L_S. Other details are given in Table I.

At the IF ω_0, the admittance matrix for ports 1, 2, and 3′ of the embedding network is

$$Y(\omega_0)=\frac{1}{Z_1}\begin{bmatrix} 1 & 0 & -1 \\ 0 & 1 & -1 \\ -1 & -1 & 2+Z_1/Z_{IF} \end{bmatrix}. \quad (12)$$

The performance of the balanced mixer of Fig. 2 was computed for the two sets of circuit parameters shown in Table I, examples 5 and 6. As in the examples of the subharmonically pumped mixer, the inductance L_S was allowed to vary to study its effect. The signal, LO, image, and IF are at 103, 100, 97, and 3 GHz. The results are shown in Figs. 8 and 9.

C. Discussion of Computed Results for Subharmonically Pumped and Balanced Mixers

The most striking difference between the subharmonically pumped mixer results in Figs. 4–7, and the balanced mixer results in Figs. 8 and 9, is the presence of large peaks in the conversion loss and noise of the former as the series inductance is varied. Examination of the LO current and voltage waveforms at the diodes shows that the largest peak (e.g. near $L_S=0.3$ nH in Fig. 4) occurs when each diode starts to conduct *twice* in each LO cycle. This second period of conduction is caused by a resonance between the diode capacitance and the inductance L_S at twice the LO frequency. Substantial signal power is then converted directly to an IF current which circulates between the diodes but is not coupled to the external IF load. In the balanced mixer the LO is near the signal frequency and no such pronounced effect is observed. The lesser peaks correspond to ringing at higher harmonics of the LO during the off-period of each diode; in most cases this ringing is not strong enough to drive the diodes into additional periods of conduction.

For the larger values of the inductance L_S considered, parametric effects due to the nonlinear diode capacitance can dominate the behavior of the mixer, causing the input and output impedances to become negative and the conversion loss to become less than unity–i.e., there is conversion gain. This is shown here in Fig. 5 for a subharmonically pumped mixer.[1] It is interesting to recall that a single-diode mixer with nonlinear capacitance can also exhibit gain, as has been demonstrated by Dragone [5]. It can be shown theoretically that a double-sideband down-converter with a sinusoidally pumped elastance can exhibit similar behavior—i.e. equal conversion gain from both sidebands, and negative input and output impedances. The reason such parametric effects are not usually observed in normal mixers is probably that the series inductance is considerably lower than required for their onset.

The effect of nonlinear diode capacitance on the subharmonically pumped mixer is demonstrated in Figs. 6 and 7: in Fig. 6 the usual capacitance variation ($\gamma=0.5$) is present, while in Fig. 7 the capacitance is independent of voltage ($\gamma=0$). The main effects are a reduction of ~2 dB in the minimum conversion loss, and a reduction of ~20 percent in the minimum mixer noise temperature, when $\gamma=0.5$. With $\gamma=0$ gain and negative impedances are not, of course, observed for any value of inductance.

In the case of the balanced mixer the effects of nonlinear diode capacitance are shown in Fig. 8 ($\gamma=0.5$) and Fig. 9 ($\gamma=0$). The lower minimum conversion loss (below 3 dB) for $\gamma=0.5$ is clearly a result of parametric effects. The higher minimum noise temperature for $\gamma=0.5$ is particularly interesting, since for the subharmonically pumped mixer (Figs. 6 and 7) the minimum noise temperature was lower for $\gamma=0.5$. It is not known whether these effects are characteristic of subharmonically pumped and balanced mixers in general, or whether they depend on the particular circuits considered. Recent experimental

[1]These results are essentially independent of whether the signal is taken as the upper sideband ω_2 or the lower sideband ω_{-2}, or whether the IF is allowed to become very low.

results [6]–[9] have shown that Mott diodes (which have low capacitance variation), operated as single-diode mixers at ~100 GHz in cryogenic receivers, have given very low noise despite relatively high conversion loss. However, studies of single-diode mixers show that the parametric effect of the nonlinear diode capacitance can either improve or degrade the mixer noise temperature, depending on the particular circuit [10], and it would not be surprising to find a similar result for two-diode mixers, whether balanced or subharmonically pumped.

III. Comments on the Necessary Number of Harmonics

In the general analysis of two-diode mixers given in Part I [1], it was assumed that an infinite number of LO harmonics and small-signal sidebands could be considered. In practice only a limited number can be used, and in this section some effects of this truncation will be discussed.

To determine the conductance and capacitance waveforms at the diodes in the examples given here, a modification of the method described in [4] was used. In the modified method the nonlinear conductance and capacitance of the diode are connected to an embedding network, which includes the series resistance of the diode and is characterized in the frequency domain by its impedance. As explained in [4], ignoring harmonics above the Mth is equivalent to assuming a finite real embedding impedance Z_0 at the higher harmonics. In a practical mixer the mean diode capacitance forms a low-impedance shunt across the embedding network for high harmonics, so the value of Z_0 should not appreciably affect the solution, provided M is large enough. For the examples given in this paper eight harmonics were used ($M=8$), and changing Z_0 by a factor of ten had negligible effect on the results.

In the small-signal and noise analysis, truncating the conversion admittance matrices of the diodes [1, eqs. (8)–(10)] is equivalent to assuming the small-signal sideband voltages δV_n at the diodes are zero for $|n|>M/2$ (M is taken as an even number for simplicity). The low impedance of the mean junction capacitance at high frequencies justifies this assumption provided M is large enough.

A word of caution based on our own experience is appropriate here. In order to work with a large number of sidebands in the small-signal and noise analysis, there is some temptation to assume that the Fourier coefficients of the conductance and capacitance waveforms, of order higher than computed in the nonlinear analysis, can be set to zero. Oversize conversion admittance matrices [1, eq. (8)] can then be formed, which have a number of zero elements. The fact that the Fourier coefficients are set to zero is tantamount to changing the conductance and capacitance waveforms in a way that may be physically quite unrealizable. As an example of this, consider the Fourier coefficients of a rectangular pulse conductance waveform. If the Fourier coefficients beyond the Mth are set to zero and the new conductance waveform constructed from the truncated series, it will contain regions of negative conductance—clearly impossible for a real diode. The negative conductance can lead to absurd results when used to determine the small-signal performance of a mixer (e.g., gain in a purely resistive mixer). By using normal-size matrices no assumptions are made concerning the higher Fourier coefficients, and this difficulty is avoided.

IV. The Attenuator Noise Model for Ideal Two-Diode Mixers

For a single-diode mixer consisting of an ideal exponential diode connected to a lossless mount, it can be shown [11] that there exists an equivalent multiport lossy network (attenuator) whose port-to-port loss and output noise are equal to those of the mixer. The temperature of the equivalent network is $\eta T/2$, where η is the ideality factor of the diode (see (3)) and T is its physical temperature. The ideal exponential diode has full shot noise but no series resistance or nonlinear capacitance, although it may have a static capacitance which can be regarded as part of the embedding network for purposes of anaylsis. In this section it will be shown that the same equivalent network also describes the ideal two-diode mixer, balanced or subharmonically pumped.

Consider a balanced or subharmonically pumped two-diode mixer consisting of two ideal exponential diodes connected to a lossless mount. The following analysis uses the equations derived in Part I [1], and all symbols and terminology used here are consistent with Part I. From [1, eq. (35)], the mean-square noise voltage developed across the IF load conductance at port $(C,0)$ of the mixer, is

$$\langle \delta V_{N(C,0)} \delta V^*_{N(C,0)} \rangle = \boldsymbol{Z}^M_{(C,0)} \boldsymbol{N} \boldsymbol{Z}^{M\dagger}_{(C,0)} \tag{13}$$

where $\boldsymbol{Z}^M_{(C,0)}$ is the output row of the mixer impedance matrix $\boldsymbol{Z}^M$ defined in [1, eq. (18)], and $\boldsymbol{N}$ is the noise current correlation matrix defined in [1, eq. (36)]. Since the diode mount is lossless, the only lossy elements in the embedding network are the source and load conductances $\mathrm{Re}[Y_k]$ shown in [1, Fig. 3]. It follows that the only nonzero elements of the correlation matrix $\boldsymbol{N}$ are

$$N_{(A,m)(A,n)} = 2qI^A_{m-n}\Delta f = 2\eta kTG^A_{m-n}\Delta f \tag{14a}$$

and

$$N_{(B,m)(B,n)} = 2qI^B_{m-n}\Delta f = 2\eta kTG^B_{m-n}\Delta f \tag{14b}$$

where G^A_k and G^B_k are the kth Fourier coefficients of the conductance waveforms of diodes A and B.

From the definitions of the embedding admittance matrix and the mixer admittance matrix [1, eqs. (13) and (14)], it follows that for the ideal two-diode mixer

$$\boldsymbol{N} = 2\eta kT\Delta f[\,\boldsymbol{Y}^M - \boldsymbol{Y}^E\,]. \tag{15}$$

Since $\boldsymbol{Z}^M = [\boldsymbol{Y}^M]^{-1}$

$$\boldsymbol{Z}^M \boldsymbol{N} \boldsymbol{Z}^{M\dagger} = 2\eta kT\Delta f[\,\boldsymbol{Z}^{M\dagger} - \boldsymbol{Z}^M \boldsymbol{Y}^E \boldsymbol{Z}^{M\dagger}\,]. \tag{16}$$

Using (13), the mean-square output noise voltage is

$$\langle \delta V_{N(C,0)} \delta V^*_{N(C,0)} \rangle = 2\eta kT\Delta f[\,Z^{M*}_{(C,0)(C,0)} - Q_{(C,0)(C,0)}\,] \tag{17}$$

where

$$\boldsymbol{Q} \triangleq \boldsymbol{Z}^M \boldsymbol{Y}^E \boldsymbol{Z}^{M\dagger}. \tag{18}$$

We next evaluate the $(C,0)(C,0)$ element of $\boldsymbol{Q}$, as required in (17). From (18)

$$Q_{(C,0)(C,0)} = \boldsymbol{Z}^M_{\text{row}(C,0)} \left[\boldsymbol{Y}^E \boldsymbol{Z}^{M\dagger} \right]_{\text{column}\,(C,0)}.$$

From [1, eq. (13)], $\boldsymbol{Y}^E$ can be partitioned into nine *diagonal* submatrices $\boldsymbol{Y}^E_{IJ}$, where I and J can be A, B, or C. Hence the (I,n) element of column $(C,0)$ of $\boldsymbol{Y}^E\boldsymbol{Z}^{M\dagger}$ is $\sum_J Y^E_{(I,n)(J,n)} Z^{M*}_{(C,0)(J,n)}$. Multiplying by row $(C,0)$ of $\boldsymbol{Z}^M$ gives

$$Q_{(C,0)(C,0)} = \sum_I \sum_n \sum_J Z^M_{(C,0)(I,n)} Y^E_{(I,n)(J,n)} Z^{M*}_{(C,0)(J,n)}$$

where I and J take the values A, B, and C, and n takes the number of each sideband $\omega_n = \omega_0 + n\omega_p$. It follows that

$$\begin{aligned} Q_{(C,0)(C,0)} = {} & \sum_I \sum_n \left| Z^M_{(C,0)(I,n)} \right|^2 Y^E_{(I,n)(I,n)} \\ & + \sum_n \left[Y^E_{(A,n)(C,n)} Z^M_{(C,0)(A,n)} Z^{M*}_{(C,0)(C,n)} \right. \\ & \left. + Y^E_{(C,n)(A,n)} Z^M_{(C,0)(C,n)} Z^{M*}_{(C,0)(A,n)} \right] \\ & + \sum_n \left[Y^E_{(B,n)(C,n)} Z^M_{(C,0)(B,n)} Z^{M*}_{(C,0)(C,n)} \right. \\ & \left. + Y^E_{(C,n)(B,n)} Z^M_{(C,0)(C,n)} Z^{M*}_{(C,0)(B,n)} \right] \\ & + \sum_n \left[Y^E_{(A,n)(B,n)} Z^M_{(C,0)(A,n)} Z^{M*}_{(C,0)(B,n)} \right. \\ & \left. + Y^E_{(B,n)(A,n)} Z^M_{(C,0)(B,n)} Z^{M*}_{(C,0)(A,n)} \right]. \end{aligned} \tag{19}$$

We now use the following facts: i) For a reciprocal embedding network $Y^E_{(I,n)(J,n)} = Y^E_{(J,n)(I,n)}$. ii) For an embedding network which is lossless except for the external load conductances (see [1, fig. 3]), all elements of the admittance matrix $\boldsymbol{Y}^E$, except $Y^E_{(C,n)(C,n)}$, are purely imaginary. In (19), therefore, the last three summations are imaginary, and so are the elements of the double summation for $I = A$ or B. Therefore,

$$\text{Re}\left[Q_{(C,0)(C,0)} \right] = \sum_n \left| Z^M_{(C,0)(C,n)} \right|^2 \text{Re}\left[Y^E_{(C,n)(C,n)} \right]. \tag{20}$$

If the IF port of the mixer is terminated in a *matched* admittance $Y_0 = G_0 + jB_0$ (see [1, fig. 3]), $Z^M_{(C,0)(C,0)} = 1/2G_0$, which is real. Also, for the lossless embedding network, $G_0 = \text{Re}[Y^E_{(C,0)(C,0)}]$. Since the mean-square output noise voltage must be real, both sides of (17) must be real, and, therefore,

$$\begin{aligned} \langle \delta V_{N_{(C,0)}} \delta V^*_{N_{(C,0)}} \rangle = 2\eta k T \Delta f \Bigg\{ & \frac{1}{2G_0} - \frac{1}{4G_0} \\ & - \sum_{n \neq 0} \left| Z^M_{(C,0)(C,n)} \right|^2 \text{Re}\left[Y^E_{(C,n)(C,n)} \right] \Bigg\}. \end{aligned} \tag{21}$$

From [1, eq. (20)], the conversion loss from sideband ω_n to IF (ω_0) is

$$L_{0,n} = \frac{1}{4 \left| Z^M_{(C,0)(C,n)} \right|^2 \text{Re}\left[Y_n \right] \cdot \text{Re}\left[Y_0 \right]} \tag{22}$$

from which, with (21), it follows that

$$\langle \delta V_{N_{(C,0)}} \delta V^*_{N_{(C,0)}} \rangle = \frac{\eta k T \Delta f}{2G_0} \left[1 - \sum_{n \neq 0} \frac{1}{L_{0,n}} \right]. \tag{23}$$

The output noise power delivered to the matched load admittance is

$$P_{N_{\text{out}}} = k\left(\frac{\eta T}{2} \right) \Delta f \left[1 - \sum_{n \neq 0} \frac{1}{L_{0,n}} \right]. \tag{24}$$

$P_{N_{\text{out}}}$ is the noise power from the mixer itself, due to shot noise in the ideal diodes, and does not include noise from the external sideband terminations—this is equivalent to holding all external resistive terminations at absolute zero temperature.

Equation (24) has exactly the same form [11] as the expression for the available noise power from a multiport lossy network whose loss from any port n to the output port 0 is $L_{0,n}$, and whose physical temperature is $\eta T/2$. We conclude, therefore, that *a two-diode mixer, using ideal exponential diodes mounted in a lossless circuit, has the same output noise as a lossy multiport network (attenuator) at temperature $\eta T/2$, whose port-to-output losses $L_{0,n}$ are the same as the corresponding conversion losses (from sidebands ω_n to IF) of the mixer.* The temperature T is the physical temperature of the diodes, and η is their ideality factor (see (3)). It is emphasized that this noise model of the two-diode mixer is valid only if the diodes have no nonlinear capacitance and zero series resistance. If the diodes have a finite static capacitance, this may be considered as part of the embedding circuit for purposes of analysis, and the attenuator noise model still applies. When the diode capacitance is voltage dependent, however, parametric effects will invalidate this analysis.

As a check on the computer program used for the examples given earlier in this paper, some simple subharmonically pumped and balanced mixer circuits, having diodes with zero series resistance and fixed capacitance ($\gamma = 0$ in (2)), were analyzed using the program, and found to have a noise temperature consistent with the attenuator noise model described above.

V. Conclusion

The simple mixer circuits of Figs. 1 and 2 have been used here to demonstrate the use of the theory given in Part I, and to study the effects of the loop inductance $(2L_S)$ and diode capacitance on the performance of two-diode mixers. Although these particular examples are somewhat idealized—practical circuits would generally be more complex, especially at the higher harmonic sideband frequencies, and skin-effect loss would be present—a knowledge of the general behavior of these simple mixers can serve as a useful guide to the designer. Their behavior is discussed in detail at the end of Section II.

The subharmonically pumped mixer was found to be much more strongly affected by the magnitude of the loop inductance than the balanced mixer. This might explain the wide variation in the reported performance of subharmonically pumped mixers built in different labs.

The theory in Part I has been used to show that a subharmonically pumped *resistive* mixer does not have inherently lower noise than a fundamental resistive mixer. The theory was applied to the case of a two-diode mixer in which the diodes are ideally exponential, having full shot noise but no series resistance or nonlinear capacitance, and in which the mixer mount is lossless. It was shown that, as in the case of the single-diode mixer, the two-diode mixer, balanced or subharmonically pumped, has a noise-equivalent lossy multiport network (attenuator) whose physical temperature is $\eta T/2$, where η is the ideality factor of the diodes. When diodes with appreciable nonlinear capacitance are used this result no longer applies.

The theory of two-diode mixers provides a basis for numerical analysis of subharmonically pumped or balanced mixers, and enables the engineer to optimize a mixer design with respect to one or more embedding circuit element values, diode parameters, LO power, or dc diode bias (if any). In some cases the embedding network may be a circuit containing lumped and/or distributed elements. When such a representation is not feasible (as, for example, in most waveguide mixer mounts, which are overmoded at harmonics of the LO), measurements on a scale model of the mount can be used to characterize the embedding network.

At present the available methods for determining the conductance and capacitance waveforms of the diodes restrict the analysis to mixers with identical diodes, and in which the embedding network is symmetrical with respect to the diodes. It is believed however that the present method of nonlinear analysis can be extended to cover the more general situation, enabling the effects of diode imbalance to be studied.

The theory can easily be extended to mixers with more than two diodes (e.g., double-balanced mixers) and will be useful for their design and analysis once a suitable nonlinear analysis is available to determine the diode waveforms.

Acknowledgment

The author thanks P. H. Siegel for his help in developing a reliable method for determining the diode waveforms, and Alison V. Smith for her assistance with the computer programming.

References

[1] A. R. Kerr, "Noise and loss in balanced and subharmonically pumped mixers: Part I—Theory," this issue, pp. 938–943.

[2] E. R. Carlson, M. V. Schneider, and T. F. McMaster, "Subharmonically pumped millimeter-wave mixers," *IEEE Trans. Microwave Theory Tech.*, vol. MTT-26, pp. 706–715, Oct. 1978.

[3] A. G. Cardiasmenos, "Low-noise thin-film downconverters for millimeter systems applications," in *1978 IEEE MTT-S Int. Microwave Symp. Dig.*, pp. 399–401, June 27–29, 1978.

[4] A. R. Kerr, "A technique for determining the local oscillator waveforms in a microwave mixer," *IEEE Trans. Microwave Theory Tech.*, vol. MTT-23, pp. 828–831, Oct. 1975.

[5] C. Dragone, "Performance and stability of Schottky barrier mixers," *Bell Syst. Tech. J.*, vol. 15, no. 10, pp. 2169–2196, Dec. 1972.

[6] M. V. Schneider, R. A. Linke, and A. Y. Cho, "Low-noise millimeter-wave mixer diodes prepared by molecular beam epitaxy (MBE)," *Appl. Phys. Lett.*, vol. 31, no. 3, pp. 219–221, Aug. 1977.

[7] R. A. Linke, M. V. Schneider, and A. Y. Cho, "Cryogenic millimeter-wave receiver using molecular beam epitaxy diodes," *IEEE Trans. Microwave Theory Tech.*, vol. MTT-26, pp. 935–938, Dec. 1978.

[8] N. Keen, R. Haas, and E. Perchtold, "A very low noise mixer at 115 GHz, using a Mott diode cooled to 20K," *Electron. Lett.*, vol. 14, no. 25, pp. 825–826, Dec. 1978.

[9] S. Weinreb, private communication of measurements at the National Radio Astronomy Observatory.

[10] P. H. Siegel and A. R. Kerr, "A user oriented program for the analysis of microwave mixers, and a study of the effects of the series inductance and diode capacitance on the performance of some simple mixer circuits," NASA Tech. Mem. 80324, Goddard Space Flight Center, Greenbelt, MD, July 1979.

[11] A. R. Kerr, "Shot noise in resistive-diode mixers and the attenuator noise model," *IEEE Trans. Microwave Theory Tech.*, vol. MTT-27, pp. 135–140, Feb. 1979.